Scaling the Primate Lateral Geniculate Nucleus: Niche and Neurodevelopment in the Regulation of Magnocellular and Parvocellular Cell Number and Nucleus Volume

Barbara L. Finlay,[1]* Christine J. Charvet,[1] Isle Bastille,[1] Desmond T. Cheung,[1] José Augusto P.C. Muniz,[2] and Luiz Carlos de Lima Silveira[3]

[1]Behavioral and Evolutionary Neuroscience Group, Department of Psychology, Cornell University, Ithaca, New York 14853
[2]Centro Nacional de Primatas, 67030-000 Ananindeua, Pará, Brasil
[3]Nucleo de Medicina Tropical and Instituto de Ciências Biológicas, Universidade Federal do Pará, 66055-240 Belém, Pará, Brasil

ABSTRACT

New stereological assessments of lateral geniculate nucleus (LGN) neuron numbers and volumes in five New World primates (*Cebus apella*, *Saguinus midas niger*, *Alouatta caraya*, *Aotus azarae*, and *Callicebus moloch*) and compiled LGN volumes for an additional 26 mammals were analyzed for a better understanding of visual system evolution. Both the magnocellular (M)- and the parvocellular (P)-cell populations scale allometrically with brain volume in primates, P cells with a significantly higher slope such that, for every increase in M neuron number, P neuron numbers more than double (ln scale; $y = 0.89x + 2.42 R^2 = 0.664$). In diurnal primates, the ratio of P to M cells was slightly but significantly higher than in nocturnal primates. For all mammals, including primates, LGN volume was unrelated to nocturnal or diurnal niche but showed marked differences in slope and intercept depending on taxonomic group. The allometric scaling of M and P cells can be related to the order of neurogenesis, with late-generated P cells increasing with positive allometry compared with the earlier-generated M cells. This developmental regularity links relative foveal representation to relative isocortex enlargement, which is also generated late. The small increase in the P/M cell ratio in diurnal primates may result from increased developmental neuron loss in the M-cell population as it competes for limited termination zones in primary visual cortex. J. Comp. Neurol. 522:1839–1857, 2014.

INDEXING TERMS: M- and P-cells; New World primate; allometry; thalamus; neuron death

The varying configuration of the visual system across mammals is a valuable source of information about what aspects of its organization are intrinsic to all visual processing and which are variable. Some features will be constrained from change or actively defended against changes across niches, organism size, and visuomotor capacities, and other features will reflect adaptive specializations at the levels of individual species, taxon, or niche. The lateral geniculate nucleus (LGN) is a structure that apposes stability and adaptation in its basic description. Its fundamental place in the visual system is stable: its principal sensory input is the retina, its output is the visual cortex, and primary visual cortex returns input to it. In addition to substantial input from other visual and multimodal cortices (Kaas et al., 1978; Harting et al., 1991), the LGN exists in a matrix of modulatory connectivity both from brainstem and from forebrain (Singer, 1977; Erisir et al., 1997). With changes in brain size and visual specializations, however, the LGN can be almost unrecognizable from one mammal to another. In nocturnal rodents and microbats, for example, the LGN presents as a single, undifferentiated cell mass with a predominant

Grant sponsor: The Conselho Nacional de Desenvolvimento Científico e Tecnológico (CNPq); Grant number: 910149/96–98; Grant sponsor: National Science Foundation; Grant number: Int-9604599 (to L.C.L.S., B.L.F.) IBN-0138113 (to B.L.F.); Grant sponsor: National Institutes of Health; Grant number: F32HD067011 (to C.J.C.).

*CORRESPONDENCE TO: Barbara L. Finlay, Department of Psychology, Cornell University, Ithaca NY 14853. E-mail: blf2@cornell.edu

Received May 17, 2013; Revised November 3, 2013;
Accepted November 7, 2013.
DOI 10.1002/cne.23505
Published online November 13, 2013 in Wiley Online Library (wileyonlinelibrary.com)

contralateral and minority ipsilateral input from the retina (Cotter, 1985; Reese, 1988). In larger visual systems across taxa (Conley et al., 1984; Cotter, 1985; Malpeli et al., 1996; de Sousa et al., 2013), details of its functional complexity become apparent in its gross morphology, with multiple layers differentiating functional groups of neurons of varying properties reflecting spatial, temporal, and spectral discriminations as well as eye of origin. In the largest brains, because of the allometric scaling properties of the relevant populations, the relative proportion of retinal input compared with cortical input becomes quite small (Finlay and Brodsky, 2006).

Information from multiple species is critical to distinguishing general aspects of visual system scaling common to all mammals from variations in the basic plan. These variations can be of two general kinds. First, "grade shifts" can be seen at large taxonomic divisions, for example, shifting neural mass toward olfactory-limbic processing vs. neocortical processing or vice versa (Reep et al., 2007). Such grade shifts can be viewed as large-scale tactical "decisions" at taxonomic boundaries on the best disposition of processing resources in a group of related species. Other adaptations may cross taxonomic boundaries and appear in individual species, such as those required for a nocturnal or diurnal niche or for particular foraging needs or social communication. The fact that "stem" mammals were primarily nocturnal (Hall et al., 2012), as were stem primates (Ross, 2000), has made understanding of visual system evolution methodologically complex, because phylogenetic samples typically come populated with large numbers of small-brained nocturnal animals and large-brained diurnal ones, with very few cases of the reverse linkage. This nonrandom assortment systematically confounds brain size with niche.

"The visual system" is not a single entity, selected to be relatively larger or smaller in accordance with functional demands. In basic brain allometry, every brain subregion and cell class can be found to have its own exponent in standard allometric equations with respect to the scaling of overall brain volume or neuron number. For example, both rods in the retina and supragranular neurons in the primary visual cortex increase in number rapidly with respect to brain volume, independent of niche ("positive allometry"), whereas the relative numbers of retinal ganglion cells decrease with respect to whole-brain size, "negative allometry" (Finlay et al., 2005; Cahalane et al., 2012). Finally, the adaptive response to the same niche in different taxa can take various forms: nocturnal rodents have relatively small eyes whereas nocturnal birds, carnivores, and primates have relatively large eyes compared with their diurnal cousins (Hall et al., 2012).

Work so far on the allometry of the visual thalamus suggests that mammals, as a group, display a "grade shift" that allocates relatively more neural mass to thalamus and forebrain vs. midbrain (Yopak et al., 2010). Within the mammalian thalamus, the LGN is the most conservative, with negative allometry, and the lateralis posterior and pulvinar complex have strong positive allometry with respect to brain volume (Armstrong, 1979, 1981; Stephan et al., 1981; Chalfin et al., 2007). Within the lateral geniculate, a variety of mammals show a distinction between two main group of neurons, alpha and beta cells in nonprimates, and magnocellular (M) and parvocellular (P) cells, which corresponds to a similar distinction in the retinal ganglion cells. P cells are physically small cells with small receptive fields and sustained responses, signaling high spatial frequency and low temporal frequency selectivity, and are relatively insensitive to spatial and temporal contrast. M cells, physically large cells with large receptive fields preferring lower spatial frequencies and higher temporal frequencies, are very sensitive to spatial and temporal contrast (Stone, 1983; Kaplan and Shapley, 1986; Shapley and Perry, 1986). For primates, a special role in trichromacy has been proposed for P cells (Shapley and Perry, 1986; Mollon, 1991). For nonprimates, alpha and beta cells are generally considered the relative counterparts of M and P cells, but the two groups differ considerably in absolute values of all parameters compared with their primate counterparts (Shapley and Perry, 1986; Silveira et al., 1994).

This article presents a stereological assessment of M- and P-cell numbers in the LGN of five New World primates (*Cebus apella*, *Saguinus midas niger*, *Alouatta caraya*, *Aotus azarae* and *Callicebus moloch*), comparing it with previous work on the scaling of M- and P-cell populations in multiple primates. In addition, we describe the scaling of the volume of the LGN across a wide variety of mammals, compiled and analyzed from a number of sources, comparing taxonomic membership and niche adaptations. This article is part of a series examining the scaling and adaptation of the visual system, featuring new data on New World primates' eye conformation (Franco et al., 2000), retina (Finlay et al., 2008), and pulvinar (Chalfin et al., 2007) and visual cortices (Kaskan et al., 2005; Cahalane et al., 2012; Charvet et al., 2013).

MATERIALS AND METHODS

The present article integrates data on neuron number and volume of the LGN in mammals from a number of sources, including 1) new stereological assessments of neuron number in New World primates from tissue processed in this laboratory, 2) the "Brain Museum" database (http://brainmuseum.org/sections/index.html; access date: January 5, 2006), and 3) brain

TABLE 1.

Species, Brain and LGN Volumes, Source, Processing, and Classification[1]

Animal	Scientific name	SO	BrVol bilat (mm^3)	LGN present bilat (mm^3)	LGN Stephan bilat (mm^3)	T	Q	N
Beaver	*Castor canadensis*	13	43,400	80.6		C	2	N
Cat	*Felis catus*	5	24,700	99.6		C	2	C
Capuchin monkey	*Cebus apella*	1	60,800	116.4	137	F	3	D
Dog (beagle)	*Canis familiaris*	13	69,500	117.9		F	1	C
Gerbil	*Meriones unguiculatus*	12	1,100	1.1		C	1	D
Gibbon	*Hylobates lar*	4,6	101,200	175		F	5	D
Gorilla	*Gorilla gorilla*	4,6	521,200	384		F	5	D
Hamster	*Mesocricetus auratus*	5	9,600	1.57		F	1	N
Harbor seal	*Phoca vitulina*	3	239,000	439.1		C	2	D
Howler monkey	*Alouatta caraya*	1	57,500	99.0	87	F	3	D
Human	*Homo sapiens*	11	1,334,900	406.7	416	P	1	D
Hyena	*Crocuta crocuta*	3	139,100	344.3		C	2	N
Kangaroo	*Macropus fuliginosus*	5	54,100	129.0		C	2	D
Lion	*Panthera leo*	3	229,500	542.5		C	2	N
Macaque	*Macaca mulatta*	2,6	91,700	190.1	158	C	2	D
Manatee	*Trichechecus manatus*	3	281,900	621.4		C	2	C
Mandrill	*Mandrillus sphinx*	2	153,900	277.2		C	2	D
Marmoset	*Callithrix jacchus*	6	6,900	23.2	25	F	3	D
Mongoose	*Cynictus penicillata*	8	9,700	79.0		C	2	D
Mongoose lemur	*Eulemur mongoz*	2	21,000	45.6		C	2	C
Mouse	Strain C57BL/6J	9	400	0.6		F	4	C
Mouse lemur	*Microcebus murinus*	10	1,700	7.52		F	4	N
Owl monkey	*Aotus* sp.	1	17,400	32.3	32	F	3	N
Paca	*Cunniculus paca*	1	31,800	22.4		F	3	N
Rat	*Rattus rattus*	5	1,800	3.8		F	1	N
Rock hyrax	*Procavia capensis*	7	15,900	61.2		C	2	D
Sea lion	*Zalophus californicus*	3	383,700	1,814.9		C	2	D
Squirrel monkey	*Saimiri scirius*	2	23,600	67.5	63	F	3	D
Tamarin	*Saguinus midas*	2	10,000	40.1	36	F	3	D
Titi monkey	*Callicebus moloch*	2	18,300	40.7	54	F	3	D
White-tailed deer	*Odocileus virginianus*	3	114,600	834.7		C	2	D
Zebra	*Equus burchelli*	3	427,900	859.6		C	2	D

[1]SO, source for brain weight value (1, this study; 2, Rowe, 1996; 3, Reep et al., 2007; 4, Armstrong, 1981; 5, Allison and Cicchetti, 1976; 6, Stephan et al., 1980; 7, Yom-Tov, 1993; 8, Gittleman, 1995; 9, Seecharan et al., 2003; 10, Bons et al., 1998; 11, Mai et al., 1997; 12, Cabana et al., 1990; 13, http://staff.washington.edu/chudler/facts.html; 08/05/2006). LGN vol present/Stephan: Reconstruction, present study vs. Stephan et al. (1980). T, tissue processing (F, frozen sections; C, celloidin; P, paraffin). Q, quantification technique (1, atlas; 2, brainmuseum; 3, this study; 4, special process for truncation; 5, volume recovered from cell number). N, niche (C, cathemeral; N, nocturnal; D, diurnal).

atlases (Dua-Sharma et al., 1970; Loskota et al., 1974; Bons et al., 1998; Morin and Wood, 2001; Paxinos, 2004) and various published works (Tables 1, 3; Chalfin et al., 2007). Two goals guided this integration; first, to ensure the comparability of the various assessments of lateral geniculate neuron number, thalamus, and brain volume from these various sources, and, second, to collect as wide a range of brain sizes and niches as possible, both across the mammalian orders and within various mammalian suborders.

Stereological determination of neuron numbers and volumes of New World monkey brains from sectioned material

Histological procedures. Samples came from animals bred or housed in the Centro Nacional de Primatas in Pará, Brazil. All animal housing and procedures complied with the principles defined in the NIH *Guide for the care and use of laboratory animals*, as certified through the IACUC at Cornell University as part of a larger study. One capuchin monkey (*Cebus apella*), two tamarin monkeys (*Saguinus midas niger*), two howler monkeys (*Alouatta caraya*), three owl monkeys (*Aotus azarae*), and one dusky titi monkey (*Callicebus moloch*) were collected from this source.

Animals were dark adapted for 30 minutes while lightly anesthetized with an intramuscular injection of a 1:4 mixture of 2% xylazine hydrochloride and 5% ketamine hydrochloride. They were then deeply anesthetized with the same mixture and perfused with a phosphate-buffered saline solution (pH 7.2). An unfixed eye was then removed. They were then perfused with 4% paraformaldehyde. Brains were dissected out and weighed. After 1–2 weeks, the brains changed to 2% paraformaldehyde and were refrigerated if extended storage was

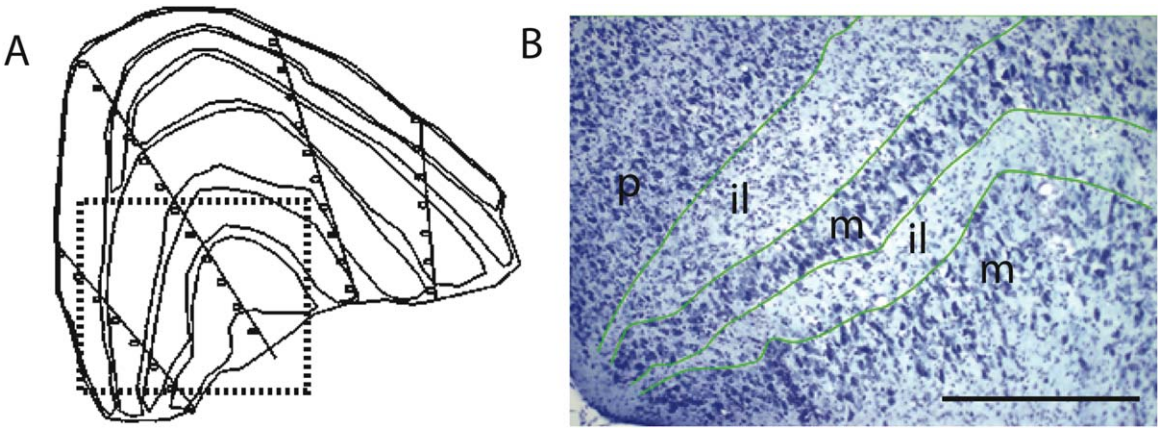

Figure 1. **A**: Schematic of coronal section of *Alouatta caraya* LGN demonstrating positioning of radial sampling probes. **B:** Photomicrograph corresponding to boxed area in A showing identification of lamina. p, Parvocellular lamina; il, intralaminar; m, magnocellular. Scale bar = 500 μm. [Color figure can be viewed in the online issue, which is available at wileyonlinelibrary.com.]

intended. For sectioning, brains were then sunk in 30% sucrose/phosphate buffer solution (0.1 M; pH 7.2) and sectioned coronally on a freezing microtome at 60 μm. Every fifth or seventh section was mounted on gelatinized slides and stained with cresyl violet.

Determination of volumes and neuron numbers were done as follows. Volumetric measurements of the LGN, thalamus, and whole brain were reconstructed in Stereoinvestigator (Neurolucida; version 5). The numbers of neurons in the LGN of the rhesus macaque have been estimated multiple times, using "assumption-based" counting methods, "unbiased" stereological methods, and hybrids (Williams and Rakic, 1988; Ahmad and Spear, 1993; Suner and Rakic, 1996; Blasco et al., 1999; Williams and Jeffrey, 2001). These methods do not deliver such discrepant results to dictate the use of one or the other, so we chose the method of Williams and Rakic (1988) in which four radial probes are placed to divide evenly the outermost and the innermost perimeters to designate counting regions (Fig. 1A), and stereological methods to determine cell numbers in probe locations. This method samples the M, P, and intralaminar divisions in each coronal section (Fig. 1B) more efficiently than random counting assignments, and the resulting data can be directly registered with the data on LGN neurogenesis, one of the ultimate goals of the study (Rakic, 1977). All counts were made at ×750 magnification. Section areas were integrated by the Cavalieri method as implemented in Stereoinvestigator and multiplied by neuronal densities per section to determine the total number of neurons per nucleus. Neuron numbers were summed into M, P, and intralaminar divisions, but, because the majority of prior studies have examined only the M and P divisions, here we discuss only those data, although intralaminar counts are included in the tabular material. Neurons are designated as M or P only by the lamina in which they reside, not in the features or size of each individual neuron, in accordance with prior literature (Figs. 1, 2). Neurons were distinguished from glia by the criteria described in earlier primate LGN studies (Williams and Rakic, 1988; Ahmad and Spear, 1993). We have undertaken no analysis of particular features or the distribution of cell sizes in the New World monkeys presented here, because these features of the primate LGN have already been addressed in detail elsewhere, most recently for catarrhine primates (de Sousa et al., 2013).

All counts were performed unilaterally and doubled to represent the volume and total number of neurons in the LGN per brain. The brains were used for multiple purposes over multiple years, so no convention was used for whether the right or left side was counted, a generality also true of the cell counts and volumes gathered from the research literature, although we note the brain side for each case we present. It should be noted that the convention, often undeclared, of presenting unilateral or bilateral LGN counts is quite variable between investigators. This can be a source of much confusion: individuals whose main interest is the visual system usually present unilateral counts, compared with those interested in brain allometry, who give bilateral counts, but not so predictably as to avoid mistakes.

Determination of LGN, thalamus, and brain volumes from literature sources

Criteria for including animals from these sources included the following. All brains had to have no fewer than five sections containing LGN complex and a minimum of 14 sections spanning the rostrocaudal extent

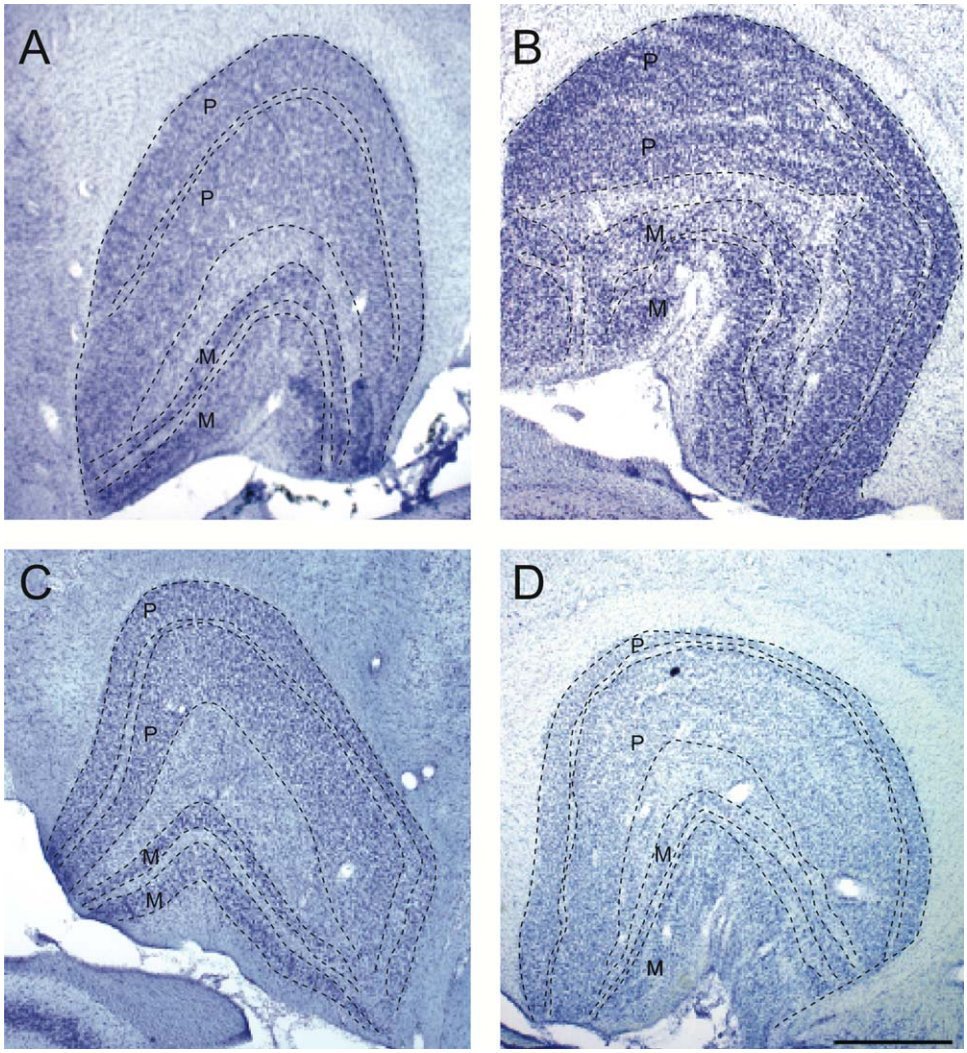

Figure 2. Coronal sections at the approximate AP midpoint of the LGN in four New World primates. **A:** *Callicebus moloch*. **B:** *Cebus apella*. **C:** *Aotus azarae*. **D:** *Alouatta caraya*. Dashed lines indicate the delineations between parvocellular and magnocellular layers as well as the delineations of the LGN. Scale bar = 1 mm. [Color figure can be viewed in the online issue, which is available at wileyonlinelibrary.com.]

of the brain. All brain images obtained from the brainmuseum.org website had to be of adequate resolution to discern the relevant detail necessary to draw the laminar boundaries of the LGN. Finally, fresh brain volumes of the specimen were required, preferably obtained from the atlas or laboratory responsible for processing the brain in question.

Images of brains obtained from brainmuseum.org were first saved as JPEG files and then either printed out and traced into NIH Image v1.61 with a Wacom 6 38-in data tablet or loaded into NIH image J 1.31. Using the scaling provided on the site, we estimated the areal extent of each section containing the LGN. With the section thicknesses obtained from the site holders, we used Cavalieri's estimator to estimate the volume of the LGN, thalamus, and brain (Table 1; quantification method Q-2).

A more detailed account of normalization of all measurements to fresh brain volumes is given by Chalfin et al. (2007). All volumes derived from sections, atlases, or web resources were corrected to represent a fraction of whole-brain volume by the following procedure. First, the volume of the entire fresh brain was divided by the volume of its serial-section-reconstructed counterpart to obtain a shrinkage correctional factor, and this was applied to the calculated LGN volume. Although all of the analyses we perform here are expressed as volumes, it is by correcting measured brain volumes to brain weights that allows comparison of the brains from diverse sources to be made (specific gravity of brain = 1.036; Stephan et al., 1981). The unusual diversity of sources for these brain measurements made it desirable to determine whether our

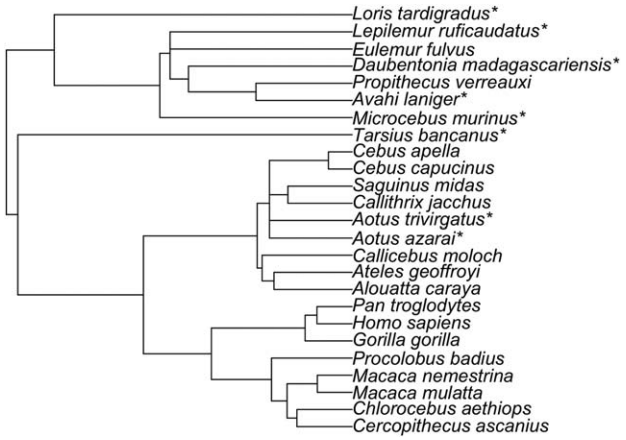

Figure 3. The phylogeny of the 25 primate species used in this study was extracted from Bininda-Emonds et al. (2007). Species with asterisks are considered to be nocturnal.

correction and quantification methods were successful in calibrating the brains to each other. Nine of the species we quantified are identical to the species, but not the individuals, examined by Stephan et al. (1981), the most widely used source in allometric studies (columns 5 and 6, Table 1), and the results can be directly compared. The convergence of the results is quite close; these measurements have been graphed by Chalfin et al. (2007).

Statistical procedures

Our overall strategy is first to examine the relationship of a feature in question, such as the numbers of M and P cells, or lateral geniculate volume to brain volume, with simple regression analysis. Once the general allometric context is established, multiple techniques, each with differing strengths and weaknesses, are used together to distinguish the differential contributions of phylogeny and niche to the allometric relationship. In the several analyses reported, we used phylogeny-generalized least squares statistics (PGLS) to obtain phylogenetically controlled slopes and residuals in R (version 2.15.0) with the Caper package. The phylogeny for mammals (Fig. 3), which includes branch lengths for the selected species, was taken from Bininda-Emonds et al. (2007). Regression parameters were found by maximum likelihood estimates (ML).

To look at the effects of nocturnality vs. diurnality, we used two methods, residual analysis and phylogenetically controlled regressions. Although residuals are often used to examine the relationship between neural traits and ecological variables and have been used specifically in analysis of the LGN (Barton, 1998), the use of residuals has limitations (Darlington and Smulders, 2001). An alternative method is to ask whether traits of interest in nocturnal primate species fall outside the 95% confidence intervals of the traits of interest of diurnal species, a phylogenetically controlled regression that we also employ, which makes the dimensions of effects clear, which are often obscured in residuals analysis.

An additional test for phylogenetic signal in data is an estimation of Pagel's λ (Pagel, 1999; Freckleton et al., 2002). The value of λ of the residuals varies between 0 and 1. A value of 1 indicates that traits vary systematically in relation to their shared ancestry (Pagel, 1999; Freckleton et al., 2002). A value of 0 indicates that the data do not have a phylogenetic structure. We report ML values of λ and we include significance tests for likelihood ratio (LR) statistics in which we compare LR scores when $\lambda = 0$ and $\lambda = 1$ (Pagel, 1999; Barton and Capellini, 2011).

RESULTS

Gross morphology of the LGN of the New World monkey

The lateral geniculate nuclei of New World monkeys do not deviate from the extensive qualitative descriptions given for the rhesus macaque. Figure 2 shows representative coronal sections from four species representing the size and niche variation examined: *Callicebus moloch* (Fig. 2A: small brain, diurnal), *Cebus apella* (Fig. 2B: large brain, diurnal), *Aotus azarae* (Fig. 2C: small brain, nocturnal), and *Alouatta caraya* (Fig. 2D: large brain, diurnal and obligatory trichromat). No features of lamination, cell size, and conformation were clearly linked with any of these variables, although the large konicellular or "intercalated" lamina is noticeably distinct in *Aotus* (Fig. 2C). The largest LGN of *Cebus apella* (Fig. 2B) shows evidence of "leaflets" within the outermost parvocellular layers previously described for the larger LGNs of macaques and great apes (de Sousa et al., 2013).

Scaling of M- and P-cell populations

New M and P counts in five New World monkeys. Plotted in Figure 4, and given in Table 2 are the numbers of M and P cells in individual monkeys of five species analyzed in this study. The more positive allometry of P cells vs. M cells seen across primates can be discerned, although the unusually high number of P cells of all three individual tamarin monkeys (*Saguinus midas niger*) obscures the overall relationship in this subset of the data. The one nocturnal monkey, *Aotus azarae*, shows no marked deviation from population numbers in M and P cells but does have a very distinct difference

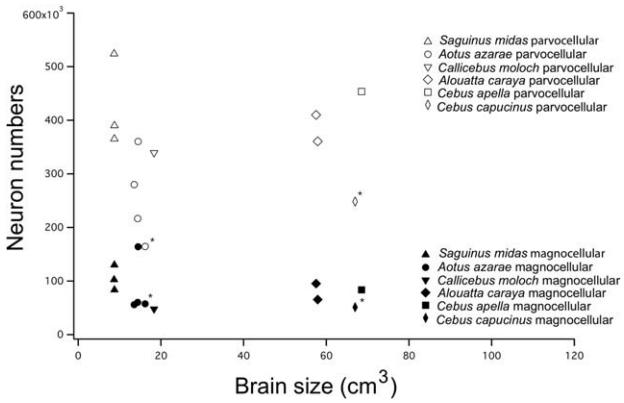

Figure 4. Numbers of M cells (solid symbols) and P cells (open symbols) plotted against brain volume for individual monkeys. Triangles, the tamarin, *Saguinus midas niger*; circles, the owl monkey, *Aotus azarae*; inverted triangles, the dusky titi, Calicebus moloch; lozenges, the howler monkey, *Alouatta caraya*; squares, the capuchin monkey, *Cebus apella*. Symbols highlighted with an asterisk are from Schulz (1976).

in the number of a third cell class that can be clearly seen in LGN sections (Fig. 2, bottom left, Table 2), which is a very large koniocellular lamina (also termed "K" or "intralaminar" or "intercalated") zone, containing approximately 380,000 cells (n = 3), five times more than *Saguinus* (approximately 75,000 koniocellular cells; n = 3). However, between the two *Alouatta caraya*, intralaminar cell numbers differed by a factor of four. This cell class has been counted infrequently, and might have high individual variability, so we note this interesting detail but cannot analyze it further, because sample availability is limited.

First we consider M and P cell numbers and scaling in primates overall. Data had been compiled for numbers of M and P cells for a variety of strepsirrhine monkeys (lemurs and lorises; Barton, 1998, reporting from the doctoral thesis of Schulz, 1967), and for haplorrhine species, a tarsier, and several New World monkeys. To this sample we add five additional species of New World haplorrhine monkeys as well as data from three Old World monkeys, three great apes, and humans bringing the total number to 25 species (Fig. 5, Table 3). A linear regression of the number of P cells vs. M cells for these 25 species without regard to brain size, phylogeny, or niche shows a strong positive allometry for P cells vs. M cells ($y = 4.5882x + 80{,}276$; $R^2 = 0.8014$). The number of M cells (unilateral) ranges from 35,000 in the smallest strepsirrhines to 400,000 in humans, whereas P cells range from 90,000 to 2,500,000 in humans, an approximately threefold greater range in P-cell numbers. The following analyses apportion this overall positive allometry to phylogenetic relatedness, brain size, and niche. For this purpose, it is useful to keep in mind the highly nonrandom distribution of features of interest: eight of the 25 species are nocturnal, and, of those eight, six are strepsirrhine primates. The two haplorhine species include the only nocturnal monkey, the New World Monkey *Aotus azarae*, and *Tarsier bancanus*, which is the unique example of the Tarsiidae and has the unusual conjunction of having both a fovea and being nocturnal. No strepsirrhine species, nocturnal or diurnal, nor *Aotus*, has a fovea.

In Figure 5A, the natural-logged values of P cells and M cells are logged against each other, and P cells (Fig. 5B) and M cells (Fig. 5C) are regressed against the natural-logged values of brain size. These phylogenetically controlled regressions are generated as described in Materials and Methods, and 95% confidence intervals for each regression equation are plotted as dotted lines. P-neuron numbers have a higher slope than M-neuron numbers with respect to overall brain size, when compared directly with each other or when each

TABLE 2.
M and P Cell Numbers of New World Monkeys in This Study

Species	Individual	Hemisphere	Body wt (g)	Sex	Br vol bilat (mm^3)	Magno unilat cells	Parvo unilat cells	Intralam unilat cells	Magno vol unilat (mm^3)	Parvo vol unilat (mm^3)
Cebus apella	CA970913	Right	2,180	M	59,900	83,500	453,600		4.89	14.60
Alouatta caraya	AC980114	Left	1,850	F	57,900	65,300	360,600	418,800	3.47	12.39
	AC970111A	Left	4,800	M	52,400	95,200	409,900	98,700	6.49	13.63
Aotus azarae	AT980115A	Left	870	M	13,500	55,900	279,900	335,700	2.48	8.15
	AA970114A	Right	520	F	14,400	60,200	216,500	276,700	2.70	7.75
	AA970115	Left	590	F	14,500	164,000	360,000	524,400	3.95	5.98
Saguinus midas	SM970108A	Right	370	M	8,800	130,100	365,200	54,400	3.09	5.90
	SM970108B	Right	440	F	8,800	83,600	390,000	75,900	2.02	7.19
	SM960111A	Left	400	F		102,600	524,000	94,900	1.78	7.24
Calicebus moloch	CM960110B	Left	910	F	18,300	47,600	339,200		1.55	7.81

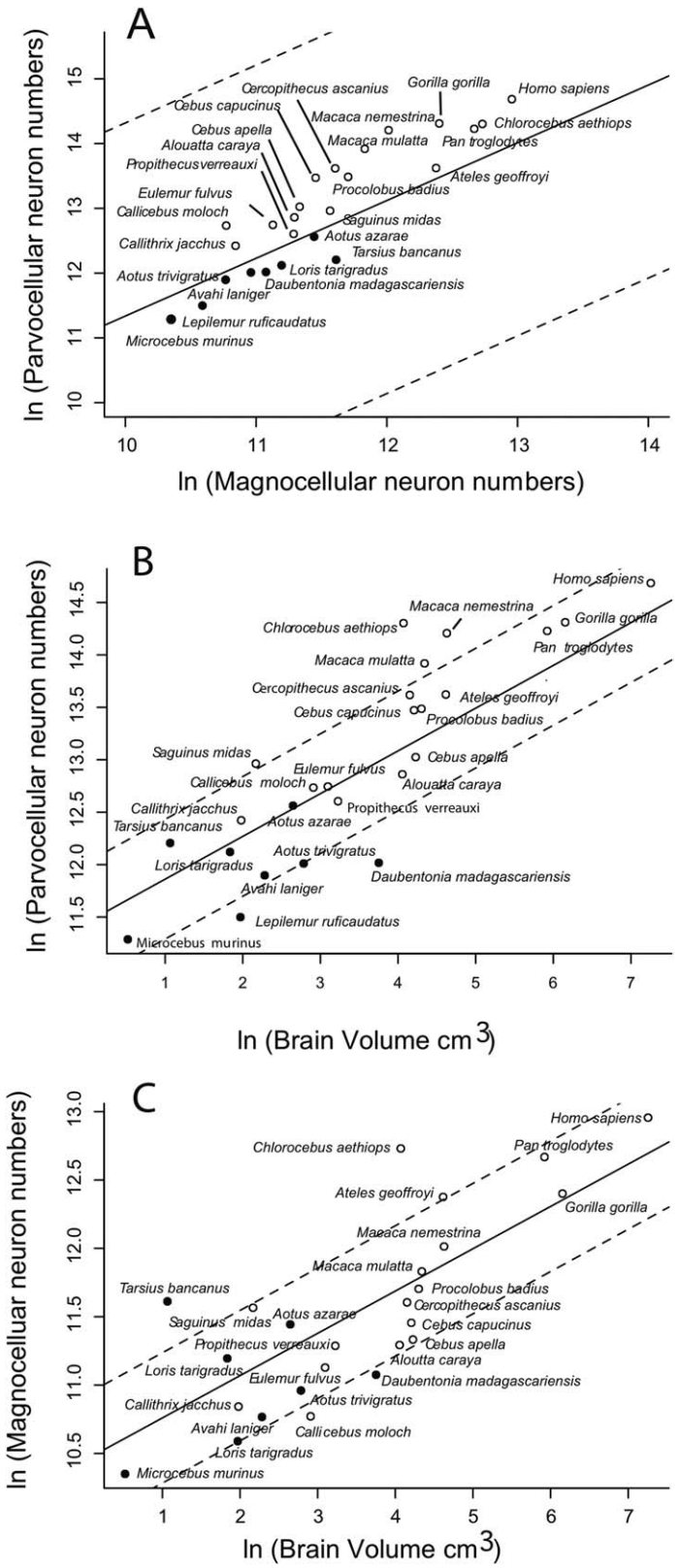

Figure 5. Phylogenetically controlled regression analyses of the number of P cells (ln) vs. M cells (ln; **A**), P cells vs. ln brain volume (**B**), and M cells vs. brain volume (**C**) for 25 primate species. Solid circles in all graphs indicate primarily nocturnal species and open circles diurnal species. Strepsirrhine primates in all graphs are *Microcebus murinus*, *Lepilemur ruficaudatus*, *Avahi aniger*, *Daubentonia madagascariensis*, *Propithecus verreuaxxi*, *Loris tardigradus*, and *Eulemur fulvus*. None of the strepsirrhine species, diurnal or nocturnal, has a foveal specialization, nor does the owl monkey, *Aotus* sp., although the nocturnal tarsier does. Confidence intervals (95%) for each regression equation are plotted as dashed lines. A: The formula for the linear regression of P-neuron number vs. M-neuron number is $y = 0.89x + 2.42$ (natural log scale). B: The formula for the linear regression of natural-logged values of P neurons vs. natural-logged values of brain size is $y = 0.41x + 11.45$. C: The formula for the linear regression of M-neuron numbers on brain size is $y = 0.31x + 10.45$.

TABLE 3.
Magno- and Parvocellular Numbers in Primates[1]

Species	Brain volume (cm^3)	Magnocellular neuron numbers	Parvocellular neuron numbers
Alouatta caraya	57.72[1]	80,259.5[1]	385,239.5[1]
Aotus azarae	14.11[1]	93,338.66[1]	285,611[1]
Aotus trivigratus	16.19[2]	57,544[3,4]	164,437[3,4]
Ateles geoffroyi	101.03[2,4]	237,137[3,4]	824,138[3,4]
Avahi laniger	9.80[2,4]	47,424[3,4]	146,893[3,4]
Callicebus moloch	18.34[1]	47,637[1]	339,275[1]
Callithrix jacchus	7.24[2,4]	51,168[3,4]	248,313[3,4]
Cebus apella	68.53[1]	83,533[1]	453,578[1]
Cebus capucinus	67.08[4]	94,406[3,4]	709,578[3,4]
Cercopithecus ascanius	63.51[2,4]	109,648[3,4]	820,352[3,4]
Chlorocebus aethiops	58.58[5]	338,000[9]	1,628,000[9]
Daubentonia madagascariensis	42.61[2,4]	64,565[3,4]	165,577[3,4]
Eulemur fulvus	22.11[2,4]	68,077[3,4]	342,768[3,4]
Gorilla gorilla	470.36[2,4]	243,000[10]	1,641,000[10]
Homo sapiens	1,415.76[6,7,11]	423,405.87[6,7,11]	2,385,393.04[6,7,11]
Lepilemur ruficaudatus	7.17[2,4]	39,719[3,4]	98,628[3,4]
Loris tardigradus	6.27[2,4]	72,778[3,4]	183,654[3,4]
Macaca mulatta	76.83[2,4,11]	137,461.09[11,12]	1,108,744.18[11,12]
Macaca nemestrina	102.32[8]	165,000[8]	1,479,000[8]
Microcebus murinus	1.68[2,4]	31,261[3,4]	79,799[3,4]
Pan troglodytes	382.10[2,4]	317,500.00[10,11]	1,511,000.00[10,11]
Procolobus badius	73.82[2,4]	121,060[3,4]	719,449[3,4]
Propithecus verreauxi	25.19[2,4]	79,799[3,4]	297,852[3,4]
Saguinus midas	8.74[1]	105,420.7[1]	426,408.33[1]
Tarsius bancanus	2.90[13]	110,408[3,4]	199,986[3,4]

[1]Superscript numbers identify source (1, this study; 2, Stephan et al., 1981; 3, Schulz, 1967; 4, Barton, 1998; 5, Barrickman et al., 2008; 6, Dorph-Petersen et al., 2009; 7, Selemon and Begovic, 2007; 8, Blasco et al., 1999; 9, Papia et al., 2010; 10, Armstrong; 1979; 11, Bush and Allman; 12, Ahmad and Spear, 1993; 13, Barton and Capellini, 2011). In some cases, brain weight values were given. These values were converted to volumes by dividing the brain weight (given in grams) by 1.036. There are two main changes made to the Barton (1998) appendix: Barton uses Stephan's brain volume for the tarsier. Stephan refers to his tarsier as *Tarsier sp*., while Schulz examines magnocellular and parvocellular neuron numbers only in *Tarsius bancanus*. We therefore picked the brain weight for *Tarsius bancanus* given by Barton and Capellini (2011). Schulz reported magnoceullar and parvocellular neuron numbers for *Lepilemur ruficaudatus*, not *Lepilemur mustelinus* as reported in Barton. Although the species name has changed, the values remain the same.

is compared separately to brain size. The slope of the linear regression of natural-logged values of P-neuron numbers vs. natural-logged values of M-neuron numbers is 0.89180 ($y = 0.89x + 2.42$; slope 95% CI $\pm$ 0.259, intercept 95% CI $\pm$ 2.98; $R^2 = 0.664$; SE = 0.13226; $t = 6.7427$; $P < 0.05$; Fig. 5A). That is, for every increase in M-neuron number, P-neuron number more than doubles. The slope of the linear regression of natural-logged values of P neurons vs. natural-logged values of brain size is 0.41 ($y = 0.41x + 11.45$; slope 95% CI $\pm$ 0.138; intercept 95% CI $\pm$ 0.57; $R^2 = 0.5093$; SE = 0.070711, $t = 5.765$, $P < 0.01$; Fig. 5B). In contrast, the slope of the linear regression of natural-logged values of M-neuron numbers vs. natural-logged values of brain size is 0.31 ($y = 0.31x + 10.45$, slope 95% CI $\pm$ 0.12; intercept 95% CI $\pm$ 0.48; $R^2 = 0.591$; SE = 4.8855; $t = 4.8855$, $P < 0.01$; Fig. 5C).

The phylogenetically controlled regression accounts for more than half of the overall variance. The phylogenetic contribution to this variance has several potential sources, including in this case "grade shifts." P- and M-cell numbers for all great apes and humans lie above the regression line, and the large majority of strepsirrhine M- and P-cell counts fall below it, with haplorrhines intermediate (Fig. 5A–C). However, because nocturnal and diurnal niche are confounded with these taxonomic categories, it is not possible to specify phylogenetic variance further. Nocturnal vs. diurnal niche appears also to be a source of variance: nocturnal primate species' data points consistently lie below the regression of M- vs. P-neuron numbers, whereas the diurnal primate species' data points have a tendency to lie above the regression. In this case, niche can be progressively unconfounded from phylogeny (Fig. 5A–C). The effect is much less obvious if either P or M neurons are considered separately (Fig. 5B,C). One statistical confirmation that nocturnal primate species have reduced numbers of parvocellular to magnocellular neurons can be derived by comparing intercepts of the linear regressions of parvocellular to magnocellular neurons vs. brain volume. The values for nocturnal primate species ($y = 0.0006x + 2.52$; slope 95% CI $\pm$ 0.02; intercept

95% CI ± 0.49) fall below the 95% confidence intervals of diurnal primate species ($y = -0.0001x + 5.36$; slope 95% CI ± 1.78; intercept 95% CI ± 0.003).

A second way to contrast the different scaling of M and P cells statistically is from residuals derived from the regressions, replicating a previous analysis with a subset of these data with this larger data set (Barton, 1998). These analyses reach statistical significance only when the ratio of the two cell types is considered, corresponding to the previous phylogenetically controlled regression analysis (Fig. 6A–C).

Finally, the maximum likelihood (ML) value of λ provides an estimate of the phylogenetic relation of species' traits and can be used to determine the extent to which P- and M-neuron numbers separately vary with phylogeny. A value of 1 indicates that traits vary in relation to shared ancestry, whereas a value of 0 indicates that the data do not have a phylogenetic structure, that is, are random, or related to a variable not identical to phylogenetic structure like niche. The ML estimates of λ derived from the natural-logged values of P neurons regressed against M neurons is 0.939 and is not significantly different from 1 (LR statistics [$\lambda = 0$] $P < 0.05$; LR statistics [$\lambda = 1$] $P > 0.05$). Similarly, the ML estimate of λ derived from the natural-logged values of the P neuron numbers regressed against brain volume is 0.758 and is not significantly different from 1 (LR statistics [$\lambda = 0$] $P < 0.05$; LR statistics [$\lambda = 1$] $P > 0.05$). By contrast, we found that the ML estimate of λ derived from the natural-logged values of M-neuron numbers regressed against brain volume is 0.330, not statistically different from 0 (LR statistics [$\lambda = 0$] $P > 0.05$; LR statistics [$\lambda = 1$] $P < 0.05$). Taken together, these findings show that P-neuron number is best predicted by the primate's phylogenetic group but that M-neuron number varies independently of phylogeny. We will argue that a single developmental mechanism, increased developmental cell death in the M-cell population, is the source of this difference.

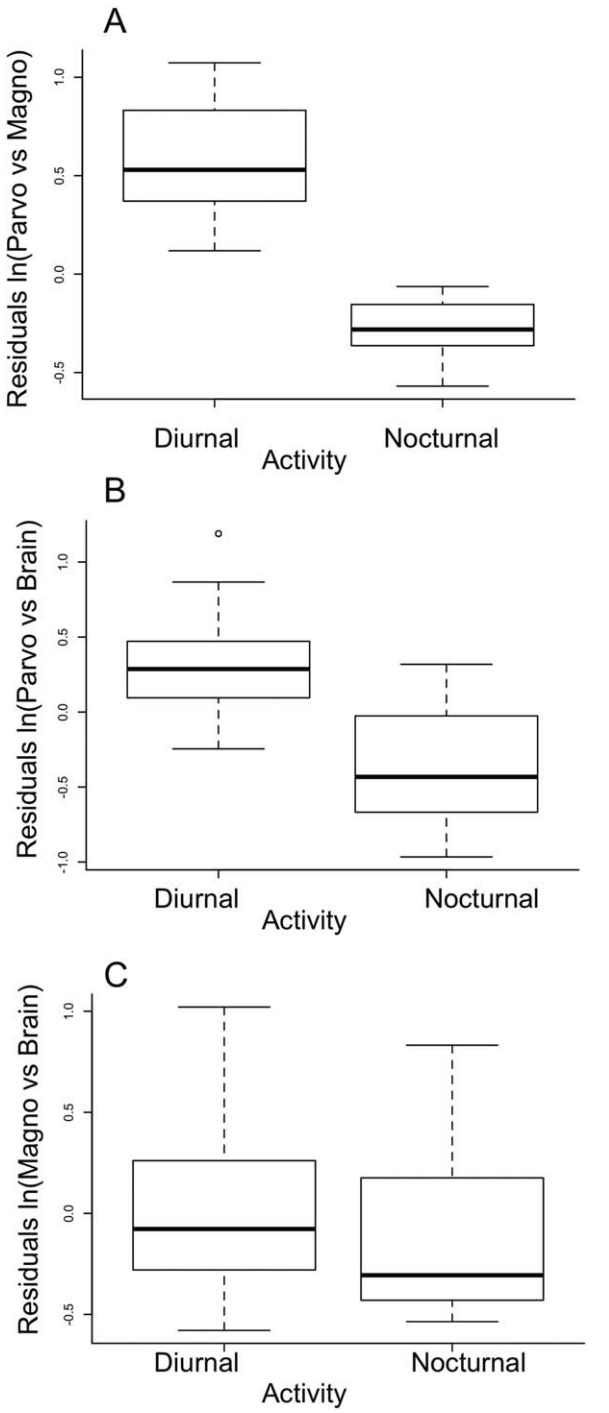

Figure 6. **A**: Mean of residuals of the ratio of P-cell numbers to M-cell numbers derived from the natural-logged regression for the diurnal vs. nocturnal primates detailed in Figure 4. **B:** Mean of residuals of P-cell numbers separately (natural-logged) as a function of brain size for the diurnal vs. nocturnal primates detailed in Figure 4. **C:** Mean of residuals of M-cell numbers separately (natural-logged) as a function of brain size for the diurnal vs. nocturnal primates detailed in Figure 4. In each graph, the solid center line is the mean, the block shows one standard deviation, and the outermost bars show the 95% confidence interval.

Volume of the LGN, placing primates in mammals generally

We used PGLS to regress the natural-logged values of the LGN volumes against the natural-logged values of the rest of the brain volume for our sample of 82 mammals (Fig. 7, Table 2). The volume of LGN correlates highly with overall brain volume ($R^2 = 0.8245$; $y = 0.91x - 6.11$; slope 95% CI ± 0.09; intercept 95% CI ± 0.47; Fig. 7A). The ML estimate of λ derived from LGN volume regressed against the rest of the brain is 1 (LR statistics [$\lambda = 0$] $P < 0.05$; LR statistics [$\lambda = 1$]

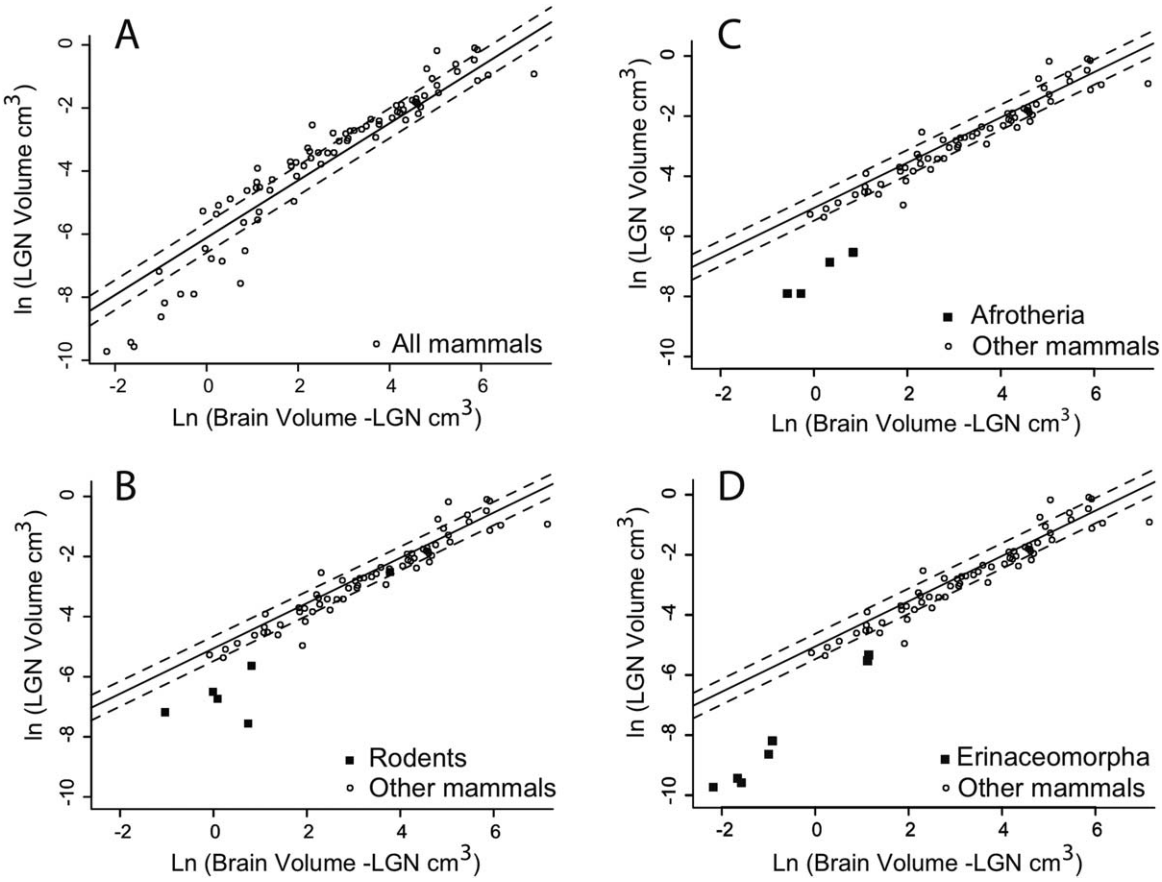

Figure 7. Representation of the relation of LGN volume to brain volume and the effect of taxonomic group. **A:** The distribution of LGN volumes vs. brain volume (both natural-logged) for the 82 mammals in this study. **B–D:** Values for each species in each of the three taxa lying outside the 95% confidence interval (dashed line) as measured by PGLS, gray dots showing the named species in each graph. Each of these taxonomic groups is plotted separately against the nonsignificant taxonomic groups for visual clarity. B: Plots rodents. C: Afrotheria, such as the hyrax and manatee. D: Erinaceomorpha, hedgehogs and shrews.

$P > 0.05$), suggesting that the correlation between LGN volume and the rest of the brain also is highly related to phylogenetic relatedness. Those species' data points lying outside of the 95% confidence intervals are mainly rodents (Fig. 7B), Afrotheria (Fig. 7C; examples are the hyrax and manatee), and hedgehogs and shrews (Fig. 7D). Bats, carnivores, and the ungulates of this sample scale with the most highly represented group, the primates, which make up about two-thirds of the total species.

We found that diurnality or nocturnality does not account for variation in LGN volumes across mammals or across primates (Fig. 8A,B). The residuals derived from the LGN vs. the rest of the brain volume regression overlap extensively across diurnal and nocturnal mammals. Moreover, the residuals derived from a linear regression of LGN volumes vs. the rest of the brain overlap extensively in diurnal and nocturnal primates (Fig. 8C,D).

DISCUSSION

Summary

To understand better the phylogenetic structure and functional significance of the scaling of the neuronal classes and volume of the LGN in primates and in mammals generally, we have added new stereological assessments of neuron number and volume in five New World primates (*Cebus apella*, *Saguinus midas niger*, *Alouatta caraya*, *Aotus azarae* and *Callicebus moloch*) and compiled or computed LGN volumes from published sources for an additional 26 mammals. The new data on LGN organization conform well to prior work on primate LGN organization, with two exceptions. One species, the tamarin, *Saguinus midas niger*, has an unexpectedly high complement of P cells, and the owl monkey, *Aotus azarae*, has a high number of koniocellular or intralaminar cells. Both M- and P-cell populations scale with brain volume in primates, P cells

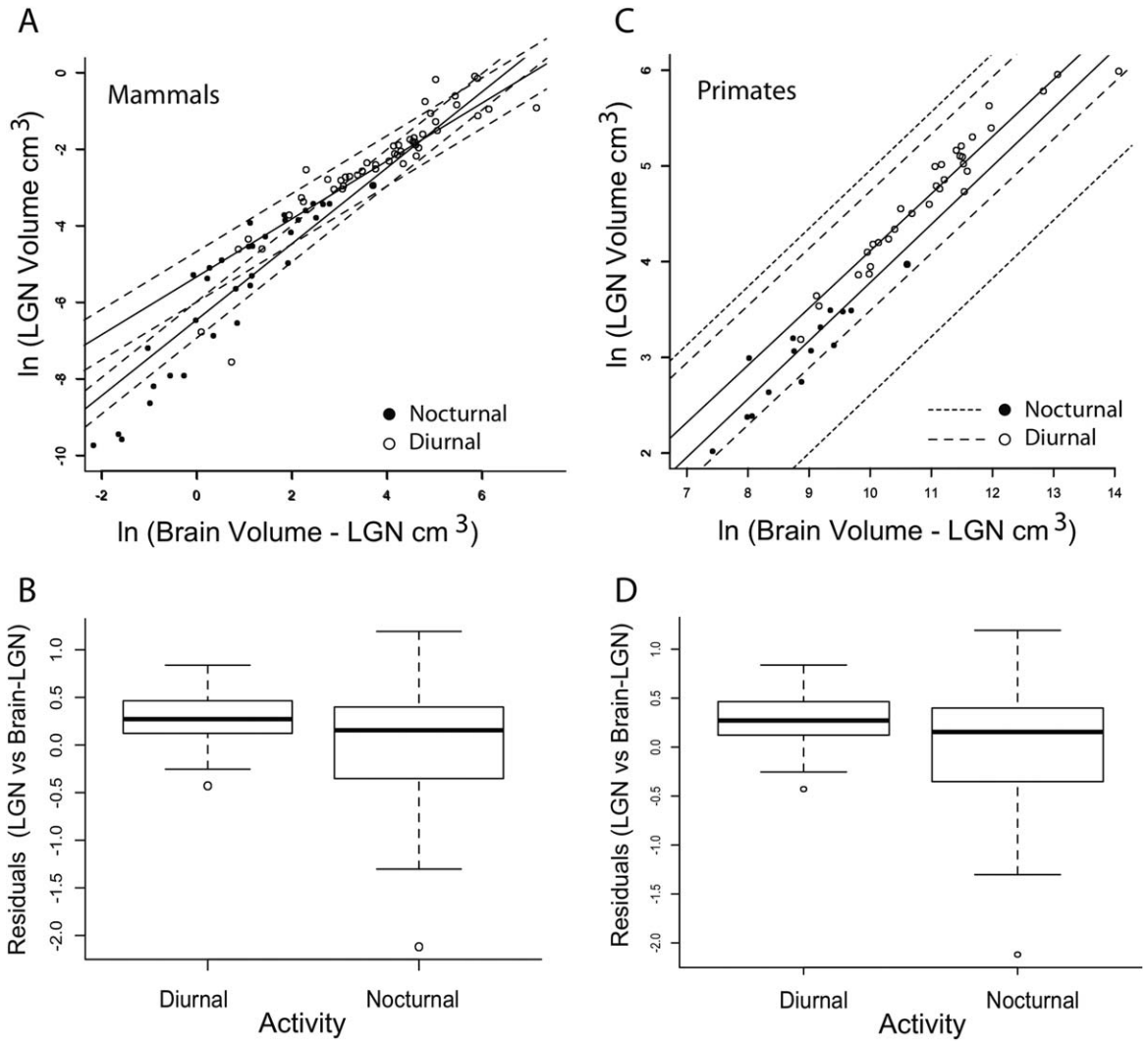

Figure 8. Relationship of nocturnal vs. diurnal life style for the relative volume of the LGN for all mammals (A,B) and for primates (C,D). **A:** Regression line for nocturnal vs. diurnal species for all mammals, and the 95% confidence interval for each, showing great overlap. **B:** Mean of residuals for nocturnal vs. diurnal LGN volumes separately (natural-logged) as a function of brain size for all mammals. In each graph, the solid center line is the mean, the block shows one standard deviation, and the outermost bars the 95% confidence interval. **C:** Regression line for nocturnal vs. diurnal species for primates, and the 95% confidence interval for each, showing great overlap. **D:** Mean of residuals for nocturnal vs. diurnal LGN volumes separately (natural-logged) as a function of brain size for primates. In each graph, the solid center line is the mean, the block shows one standard deviation, and the outermost bars the 95% confidence interval.

with a higher slope. In diurnal primates, the ratio of P to M cells was significantly higher than in nocturnal primates. Across primates and all mammals, however, the overall volume of the LGN was unrelated to nocturnal or diurnal niche. Phylogenetically, the allometry of LGN volumes broke down into two general groups, with primates, carnivores, bats, and ungulates possessing a relatively large LGN, increasing with a low slope with respect to brain volume, whereas a second group of rodents, hedgehogs, shrews, and hyraxes have relatively small LGNs scaling up steeply with brain size.

Methodological issues in the quantification of neuronal number and structure volumes

The consistency of assessments of geniculate neuron numbers and volumes is impressively consistent across studies, considering the diversity of sources (Table 3) used to generate the neuronal numbers and volumes graphed in Figures 4 and 6, all studies using various versions of stereological techniques applied to sectioned material. We attempted to include all possible sources of data in this analysis but at this point have omitted one source, studies using the "isotropic fractionator" method in which gross brain regions are dissected, homogenized, and dissociated, and neurons

are distinguished by immunohistochemistry and counted microscopically (Herculano-Houzel and Lent, 2005; Collins et al., 2013). Reported LGN neuron numbers appear markedly higher in these studies than in other studies. For example, Collins et al. (2013) report unilateral neuron numbers in the LGN of *Macaca mulatta* of 3,250,000 (n = 2) compared with a mean of 1,400,000 (n = 13) reported by Williams and Rakic (1988) or 1,465,000 (n = 7) by Ahmad and Spear (1993). For *Callithrix jacchus*, Collins et al. report 780,000 neurons compared with 300,000 (Schultz, 1967), and for *Aotus* they report 970,000 neurons compared with 633,000 (this study). Figure 9A,B plots LGN volume with respect to brain volume and LGN neuron number with respect to LGN volume separately to identify the sources of the variance better. The fractionator studies (fractionator, circles; stereology, lozenges) include five strepsirrhines (*Galago moholi*, *Otolemur garnetti*, *Eulemur mongoz*, *Lemur catta*, and *Propithecus verreauxi*) and five haplorrhines (*Callithrix jacchus*, two *Aotus* sp., *Macaca mulatta*, and *Papio cynocephalus*). Four animals overlap in the current data set (gray symbols; *Callithrix*, *Aotus*, *Propithecus*, and *Macaca*). Seven additional primate species whose range of brain sizes overlap the fractionator sample are also plotted to establish the baseline better (*Cebus apella*, *Allouatta caraya*, *Mandrillus sphinx*, *Microcebus murinus*, *Saimiri sciureus*, *Sangunius midas*, and *Callicebus moloch*). Figure 9A shows that reported LGN volumes are systematically higher in the fractionator studies, in cases three times more, such as for *Callithrix* and *Macaca*. For any given LGN volume (Fig. 9B), the fractionator studies also report higher neuron numbers, although this difference is somewhat more variable. One possible distinction of importance is that all the fractionator studies include the intralaminar zone or koniocellular zone, but only some of the stereology studies do (in the present comparison, *Aotus* and *Macaca* include all zones in both types of studies). The relative difference in cell density of this small volume compared with the M and P lamina is not very large (Fig. 2), however, and seems unlikely to account for the large discrepancy. A prior comparison of fractionator and stereological techniques in isocortex volume and neuron number also showed occasional marked deviations in volumes but no evidence of higher neuron number per volume (Charvet et al., 2013). The occasional notable discrepancy of a single individual in a species or a single species seen in allometric investigations of the visual system discussed previously should of course be taken into account, but the differences in the studies appear to be systematic, not due to single individuals. Given the convenience of the isotropic fractionator method, more effort to establish its comparability to stereological techniques, for example, by sectioning a dissected LGN to assess any extra tissue included, and by comparing the counts obtained from sectioned material vs. dissociated cells in two hemispheres from the same animal, would seem very desirable.

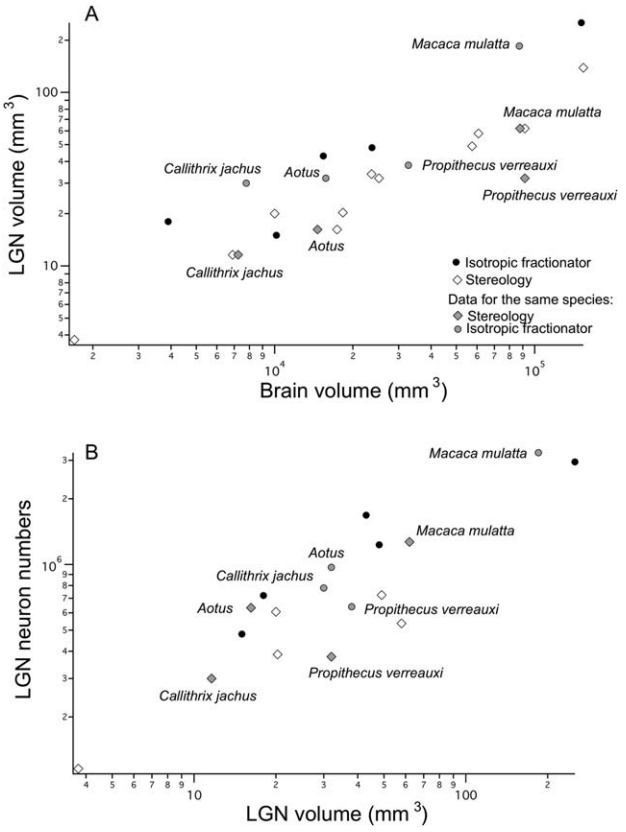

Figure 9. **A**: Comparison of data using the isotropic fractionator (circles) and stereological estimates (lozenges) show that the LGN volumes measured are systematically higher for the isotropic fractionator, considering both identical species assessed by both techniques (gray symbols) and the overall scaling of LGN volumes of primate brains in this size range. **B:** LGN neuron number vs. LGN volumes are also reported to be greater with the use of the isotropic fractionator method compared with standard stereological estimates. Data for *Macaca mulatta* are from Ahmad and Spear (1993). Data are plotted directly from Collins et al. (2013, Table 1).

Scaling and structure of the LGN

In mammals and vertebrates generally, the visual system is one of the more predictable and conservative elements of the brain (Fernald, 2001; Finlay et al., 2011). The essential problems of transduction and image analysis and the general functions of vision do not greatly change from shark to primate, resulting in eyes and retinas with very comparable lists of elements and a conserved pattern of projection on multiple targets in the di- and mesencephalon. Although transitions

from nocturnal to diurnal niches typify a number of large evolutionary transitions (Jerison, 1973; Ross, 2000) and although these transitions are associated with the most pervasive overall brain change seen in vertebrates, the relatively independent variation of olfactory-limbic structures from the rest of the brain (Jerison, 1973; Yopak, 2011; Finlay et al., 2011), visual structures for the most part scale robustly with the rest of the brain. Visual structures correlate strongly with the entire isocortex and do not dissociate themselves as a system in the way that the olfactory bulb and its central targets are apparently able to do. Within this large frame, however, interesting variations of many types can be seen.

In considering phylogenetic groups, the scaling of the relative volume of the LGN across mammals mirrors our previous report of the lateralis posterior–pulvinar complex (Chalfin et al., 2007), although mammalian phylogeny has undergone some revision in the intervening time (see, e.g., Song et al., 2012). Shrews, hedgehogs, hyraxes, and rodents generally of small body and brain size (excepting the manatee) have a relatively small LGN, which increases in size sharply with brain size, whereas primates (one branch of "*Euarchontoglires*,"); the other branches of rodents, lagomorphs, and some shrews; and "*Laurasiatheria*," comprising carnivores, marine mammals, bats, and various ungulates, have a larger base LGN volume, which increases at a slow rate with brain size, reflected in the intercepts of their corresponding regression equations. The LGN volumes of Afrotheria, rodents, and Erinaceomorpha fall below the 95% CI of that found of other mammals. This distribution suggests two independent adaptations converging on this particular allometry, once in the Laurasiatherians and again in primates, both of which include those mammals with the highest acuity and most well developed chromatic vision, although the groups are certainly not limited to mammals of that kind, notably the bats.

In considering the thalamus generally, these results confirm and amplify a pattern that has been observed across various mammals: the primary sensory nuclei of the thalamus, the LGN, the medial geniculate nucleus of the auditory system, and the ventrobasal and ventroposterolateral complex of the somatosensory system (all those nuclei projecting to primary sensory cortices) scale with a markedly low slope compared with those nuclei such as the lateralis posterior–pulvinar complex that project to nonprimary parietal or temporal or frontal regions (Armstrong, 1979, 1981; Finlay et al., 2001). This persistent difference in scaling is echoed in (and very likely directly produced by) the relative time of origin of various thalamic nuclei across all mammals examined thus far, where these primary sensory nuclei start and complete neurogenesis first in development, whereas the nuclei projecting to secondary cortical regions start and complete their neurogenesis later, the general pattern of "late equals large" (Clancy et al., 2001; Workman et al., 2013).

This evolutionary "reluctance" to increase the numbers of primary sensory projection neurons brings up a functional consideration that is rarely considered in brain allometry, in which the basic theory of "proper mass," that the brain should allocate more neurons and volumes to those sensory or motor systems in which a species is thought to specialize, is applied wholesale to all elements of that system (see, e.g., Barton, 1998; Clark et al., 2001; Krubitzer et al., 2011). Particularly for the primary geniculocortical system, "compression" (representing available information in the smallest number of transmission units, i.e., cells or axons) or "sparsification" (representing available information in the smallest number of active transmission units, a form of redundancy reduction) of the information represented in the retinal array appears to be a primary step in analysis, reducing the redundancy and activity of its numbers of channels to the minimal level adequate to represent faithfully the spatial and temporal acuity that the retinal array can measure (Field, 1994; Olshausen and Field, 1996). Therefore, although adding more elements to higher processing levels, where basic sensory information can be recombined with other derived sources of information, may be of great potential benefit, adding them at levels where reduction of dimensionality is the goal may be maladaptive or at best nonfunctional.

Regular appearance of outliers

The quest to produce general explanations of patterns in the brain and evolution produces a variation of the "file cabinet effect," in which failures to replicate or unpredicted variations are ignored or unpublished. Work quantifying the primate visual system alone has produced a long catalog of these phenomena. The relative sizes of cortical areas may vary widely from one individual to the next (Van Essen et al., 1984, 2012). The relative concentration of cones in the fovea may be quite low in about one monkey in five or six, across several species (Franco et al., 2000). The distribution of medium- and long-wavelength opsin-sensitive cells may be wildly variable in proportion in the human fovea yet unaccompanied by perceptual sequelae (Neitz et al., 2002). The howler monkey, *Alouatta caraya*, whose "typical" LGN is reported here, is an unusual obligatory trichromat among New World monkeys (Kainz et al., 1998) and has twice the density of cones in its fovea

as any other anthropoid monkey or ape, with as yet no known superior spatial or chromatic sensitivity (Franco et al., 2000). The fact that neuroanatomical information from primates outside of common laboratory species will always come from a limited number of individuals underscores the need for caution in the interpretation of particular cases.

To these outliers we add two more. The owl monkey has a very unusual number of koniocellular neurons, four times that of similarly sized monkeys, in a lamina that appears unusually well-defined compared with other laminae of New World monkeys (Fig. 2). In macaques, this lamina receives input from a number of retinal ganglion cell types, but the one specific to the lamina has been identified as the "blue-on" class. In monochromat *Aotus*, however, it is the blue opsin specifically that is absent. *Saguinus midas*, the golden- or red-handed tamarin, has an unusual number of parvocellular neurons, twice that expected. It is a small monkey with a diet and niche typical of a variety of New World primates, its most unusual feature perhaps being male parental care, which would seem irrelevant to P-cell numbers (Rylands and Mittermaier, 2009). In looking at all individual variation in our entire group of smaller-brained New World monkeys, it appears that the total number of LGN cells is reasonably constant, although proportions of subtypes vary. LGN cells are thought to arise from a single pool, M before P (Rakic, 1977), so perhaps such zero-sum reallocations might arise from changing timing or changing specification of neuron subclasses from a single pool of progenitors.

Elevated P-/M-cell ratios in diurnal primates: a neurodevelopmental account

Overall, the volume of the LGN is not related to nocturnal or diurnal niche either in mammals overall or in primates. Across niches, the relative numbers of P cells vs. M cells is first explained by a proliferation pattern common to all primates: P cells increase in number at a higher rate with brain size, consistent with "late equals large." In LGN neurogenesis, M cells are produced before P cells (Rakic, 1977), allowing the P-cell population a significantly longer time to proliferate in larger brains (Finlay et al., 2001).

The relative numbers of P cells vs. M cells are elevated even more in diurnal primates than the basic P/M allometry in primates overall, however, and here we confirm the report of Barton (1998) with our extended data set. As in his analysis, the change in neuron number is small, only marginally significant if each cell group is considered independently, and appears more strongly when unusual normalization procedures are applied. The account Barton gives of this is that the increased number of P cells is an adaptation specifically in diurnal primates for increased spatial and chromatic acuity, useful for folivory and frugivory. Because retinally based spatial and chromatic acuity remains unusually constant over the anthropoid primates, which provide most of this effect, and because the primate visual system keeps the absolute size of the fovea constant (Franco et al., 2005) and permits only the lowest variation in retinal ganglion cell number (Finlay et al., 2008) and lateral geniculate cell number (this study), however, there is good reason to be suspicious of the automatic application of the idea that more LGN neurons are an adaptation for better processing. Particularly in the chromatic domain, the visual psychophysics of monkeys and humans are spectacularly unresponsive to differences in the number and distribution of peripheral receptors (Williams et al., 1993; Neitz et al., 2002; Mancuso et al., 2009). In addition, as mentioned above, one of the major functions of the primary sensory thalamocortical connection is thought to be sparsification, reduction of the dimensionality of retinal information (Olshausen and Field, 1996).

Here we advance an argument for the difference in neuron numbers related to the early organization of the visual system primates, an argument that accounts for some heretofore unexplained observations, particularly one by Williams and Rakic (1988) concerning inhomogeneity of cell death in the macaque LGN in early development. An early debate about primary visual cortex was whether the "magnification factor" of the cortex, (the cortical area, volume or number of cells devoted to some aspect of the retinal representation) represented the increased density of ganglion cells in central retina, faithfully translating retinal cell number to cortical area, or whether the cortex overrepresents the fovea (Wässle et al., 1990, 1991). The debate was eventually resolved in favor of overrepresentation (Perry and Cowey, 1985; Silveira et al., 1989; Picanço-Diniz et al., 1991; Azzopardi and Cowey, 1993; Silveira et al., 1993). A very recent study in the marmoset (Chaplin et al., 2013) confirmed the same. This debate can be reframed in terms of the topographic distribution of P and M cells. P retinal ganglion cells are very concentrated in the fovea and in the periphery, whereas M cells, although they also peak in the fovea, have more than double the proportion in the far periphery (Perry and Silveira, 1988; Silveira and Perry, 1991; de Lima et al., 1996; Yamada et al., 1996, 2001). When these two populations project to the cortex, via the lateral geniculate, they project to the same terminal cells. That is, there is only one representation of visual field topography in the cortex, not a foveal overrepresentation for P cells and a

more even distribution elsewhere for M cells. How is this accomplished?

In the retina, maturation begins in the center of the retina and moves to the periphery (Robinson, 1987), an effect that is exaggerated in the particular case of the development of the primate fovea (for review see Hendrickson, 2005; Finlay et al., 2005). The P cells of the fovea have a numerical advantage in the representation of the visual field and a temporal advantage in the establishment of that representation in the LGN and cortex. When the M cells, disproportionately representing the periphery, attempt to establish territory in the cortex, the amount of area remaining for them to establish their projection and remain in register with the P-cell map is likely to be very small. During the period when LGN cells are competing to establish connections in the cortex in the macaque monkey, neuron death is distinctly elevated in the prospective M-cell population and in the part of that population that represents the retinal periphery (Williams and Rakic, 1988). In the nocturnal owl monkey (Dyer et al., 2011) and nocturnal strepsirrhines, there is no fovea, and the interactions of the spatial and temporal gradients are much diminished as the P-cell gradient is relaxed (Silveira et al., 1994), so we might suspect much less differential neuron loss.

Thus, the small difference in the relative numbers of P and M cells in diurnal foveate monkeys may be an epiphenomenon of the competition of these two populations for cortical area, induced by the mechanisms that produce foveas, and the change in the P/M ratio should be attributed to a relative loss of M cells, not gain of P cells. This competition could be a part of the mechanism by which the P-cell population enjoys a greater functional contribution to the visual cortex beyond its numbers alone, a putative adaptation, but any direct benefit of this minor increase has not been demonstrated. In fact, a modest decrease in the M cell population in diurnal primates may have no functional significance at all.

Finally, one interesting feature of the linked allometry of the retina, LGN, and cortex is that relative specialization of the fovea is developmentally linked to the volume of the cortex: increasing developmental duration produces a fovea with a smaller retinal angle and a larger cortex. Having a fovea is a computationally expensive solution to vision: concentrating processing resources in a tiny region of the retina requires that information about particular environments be registered, integrated over multiple views, and remembered to guide future vision. The fovea appears to be under strong absolute size constraints in the primate lineage, so the visual angle the fovea subtends decreases somewhat in larger eyes (Franco et al., 2000). In diurnal primates, relatively larger eyes are correlated with relatively larger brains (including visual cortex). This developmental linkage might thus automatically provide necessary processing resources for increasing gaze-to-gaze integration. This relationship might have a privileged, central role in gaze and "joint regard" in the social organization of primates.

ACKNOWLEDGMENTS

Multiple people contributed to the long-term project that includes this article. We thank Justin Crowley, Elizabeth S. Yamada, Michael Hersman, and David Ziegler for their help with the initial phases of this project; Francinaldo L. Gomes, Walter Augusto de Carvalho, Edna Christina S. Franco, Cezar A. Saito, and Brandon Chalfin for general assistance; and Jeremy Yost and the very helpful staff at the Centro Nacional de Primatas for technical assistance.

CONFLICT OF INTEREST STATEMENT

None of the authors has any financial or personal interests in individuals or institutions that could inappropriately influence this work.

ROLE OF AUTHORS

All authors had full access to all the data in the study and take responsibility for the integrity of the data and the accuracy of data analysis. Study concept and design: BLF, DTC, JAPCM, LCLS. Acquisition of data: B.LF, IB, DTC. Analysis and interpretation of data: BLF, CJC, IB, DTC, LCLS. Drafting of the manuscript: BLF, CJC, DTC, IB. Critical revision of the manuscript for intellectual content: BLF, CJC, LCLS. Statistical analysis: DTC, CJC. Obtained funding: BLF, JAPCM, LCLS. Administrative, technical, and material support: JAPCM. Study supervision: BLF, JAPCM, LCLS.

LITERATURE CITED

Ahmad A, Spear PD. 1993. Effects of aging on the size, density, and number of rhesus monkey lateral geniculate neurons. J Comp Neurol 334:631–643.

Allison T, Cichetti DV. 1976. Sleep in mammals: ecological and constitutional correlates. Science 194:732–734.

Armstrong E. 1979. Quantitative comparison of the hominoid thalamus. I. Specific sensory relay nuclei. Am J Phys Anthropol 51:365–382.

Armstrong A. 1981. A quantitative comparison of the hominoid thalamus. IV. Posterior association nuclei—the pulvinar and lateral posterior nucleus. Am J Phys Anthropol 55:369–383.

Azzopardi P, Cowey A. 1993. Preferential representation of the fovea in the primary visual cortex. Nature 361:719–721.

Barrickman NL, Bastian ML, Isler K, van Schaik CP. 2008. Life history costs and benefits of encephalization: a

comparative test using data from long-term studies of primates in the wild. J Hum Evol 54:568–590.
Barton RA. 1998. Visual specialization and brain evolution in primates. Proc Biol Sci 265:1933–1937.
Barton RA, Capellini I. 2011. Maternal investment, life histories, and the costs of brain growth in mammals. Proc Natl Acad Sci U S A 108:6169–6174.
Bininda-Emonds OR, Cardillo M, Jones KE, MacPhee RD, Beck RM, Grenyer R, Price SA, Vos RA, Gittleman, JL, Purvis A. 2007. The delayed rise of present-day mammals. Nature 446:507–512.
Blasco B, Avendano C, Cavada C. 1999. A stereological analysis of the lateral geniculate nucleus in adult Macaca nemestrina monkeys. Vis Neurosci 16:933–941.
Bons N, Silhol S, Barbie V, Mestre-Frances N, Albe-Fessard D. 1998. A stereotaxic atlas of the grey lesser mouse lemur brain (Microcebus murinus). Brain Res Bull 46:1–173.
Cabana T, Jolicoeur P, Baron G. 1990. Brain and body growth and allometry in the Mongolian gerbil (Meriones unguiculatus). Growth Dev Aging 54:23–30.
Cahalane DJ, Charvet CJ, Finlay BL. 2012. Systematic, balancing gradients in neuron density and number across the primate isocortex. Front Neuroanat 6:28. doi 10.3389/fnana.2012.00028.
Chalfin BP, Cheung DT, Muniz JAPC, Silveira LCL, Finlay BL. 2007. Scaling of neuron number and volume of the pulvinar complex in New World primates: comparisons with humans, other primates and mammals. J Comp Neurol 504:265–274.
Chaplin TA, Yu H-H, Rosa MGP. 2013. Representation of the visual field in the primary visual area of the marmoset monkey: magnification factors, point-image size, and proportionality to retinal ganglion cell density. J Comp Neurol 521:1001–1019.
Charvet CJ, Cahalane DJ, Finlay BL. 2013. Systematic, cross-cortex variation in neuron numbers in rodents and primates. Cereb Cortex doi 10.1093/cercor/bht214.
Clancy B, Darlington RB, Finlay BL. 2001. Translating developmental time across mammalian species. Neuroscience 105:7–17.
Clark DA, Mitra PP, Wang SSH. 2001. Scalable architecture in mammalian brains. Nature 411:189–193.
Collins CE, Leitch DB, Wong P, Kaas JH, Herculano-Houzel S. 2013. Faster scaling of visual neurons in cortical areas relative to subcortical structures in non-human primate brains. Brain Struct Funct 218:805–816.
Conley M, Fitzpatrick D, Diamond I. 1984. The laminar organization of the lateral geniculate body and the striate cortex in the tree shrew (Tupaia glis). J Neurosci 4: 171–197.
Cotter JR. 1985. Retinofugal projections of the big brown bat, Eptesicus fuscus and the neotropical fruit bat, Artibeus jamaicensis. Am J Anat 172:105–124.
Darlington RB, Smulders TV. 2001. Problems with residual analysis. Anim Behav 62:599–602.
de Lima SMA, Silveira LCL, Perry VH. 1996. Distribution of M retinal ganglion cells in diurnal and nocturnal new world monkeys. J Comp Neurol 368:538–552.
de Sousa AA, Sherwood CC, Hof PR, Zilles K. 2013. Lamination of the lateral geniculate nucleus of catarrhine primates. Brain Behav Evol 81:93–108.
Dorph-Petersen KA, Caric D, Saghafi R, Zhang W, Sampson AR, Lewis DA. 2009. Volume and neuron number of the lateral geniculate nucleus in schizophrenia and mood disorders. Acta Neuropathol 117:369–384.
Dua-Sharma S, Sharma K, Jacobs H. 1970. The canine brain in stereotaxic coordinates: full sections in frontal, sagittal, and horizontal planes. Cambridge, MA: MIT Press.
Dyer MA, Martins R, da Silva Filho M, Muniz JA, Silveira LCL, et al. 2009. Developmental sources of conservation and variation in the evolution of the primate eye. Proc Natl Acad Sci U S A 106:8963–8968.
Erisir A, VanHorn SC, Sherman SM. 1997. Relative numbers of cortical and brainstem inputs to the lateral geniculate nucleus. Proc Natl Acad Sci U S A 94:1517–1520.
Fernald RD. 2000. Evolution of eyes. Curr Opin Neurobiol 10: 444–450.
Field DJ. 1994. What is the goal of sensory coding? Neural Comput 6:559–560.
Finlay BL, Brodsky PB. 2006. Cortical evolution as the expression of a program for disproportionate growth and the proliferation of areas. In: Kaas JH, Krubitzer LA, editor. Evolution of nervous systems. Oxford: Academic Press. p 73–96.
Finlay BL, Darlington RB, Nicastro N. 2001. Developmental structure in brain evolution. Behav Brain Sci 24:263–307.
Finlay BL, Silveira LCL, Reichenbach A. 2005. Comparative aspects of visual system development. In: Kremers J, editor. The structure, function and evolution of the primate visual system. Hoboken, NJ: John Wiley & Sons. p 37–72.
Finlay BL, Franco EC, Yamada ES, Crowley JC, Parsons M, et al. 2008. Number and topography of cones, rods and optic nerve axons in New and Old World primates. Vis Neurosci 25:289–299.
Finlay BL, Hinz F, Darlington RB. 2011. Mapping behavioral evolution onto brain evolution: the strategic roles of conserved organization in individuals and species. Philos Trans R Soc Lond B Biol Sci 366:2111–2123.
Franco ECS, Finlay BL, Silveira LCL, Yamada ES, Crowley JC. 2000. Conservation of absolute foveal area in New World monkeys–a constraint on eye size and conformation. Brain Behav Evol 56:276–286.
Freckleton RP, Harvey PH, Pagel M. 2002. Phylogenetic analysis and comparative data: a test and review of evidence. Am Nat 160:712–726.
Gittleman JL. 1995. Carnivore brain size, behavioral ecology and phylogeny. J Mammol 67:23–36.
Hall MI, Kamilar JM, Kirk EC. 2012. Eye shape and the nocturnal bottleneck of mammals. Proc Biol Sci 279:4962–4968.
Harting JK, Huerta MF, Hashikawaw T, van Lieshout DP. 1991. Projection of the mammalian superior colliculus upon the dorsal lateral geniculate nucleus: organization of tectogeniculate pathways in nineteen species. J Comp Neurol 304:275–230.
Hendrickson A. 2005. Organization of the adult primate fovea. In: Penfield and Provis, editors. Macular degeneration. New York: Springer.
Jerison HJ. 1973. Evolution of the brain and intelligence. New York: Academic Press.
Kaas JH, Huerta MJ, Weber JJ, Harting JK. 1978. Patterns of retinal terminations and laminar organization in the lateral geniculate nucleus of primates. J Comp Neurol 182: 517–554.
Kainz PM, Neitz J, Neitz M. 1998. Recent evolution of uniform trichromacy in a New World monkey. Vis Res 38:3315–3320.
Kaplan E, Shapley RM. 1986. The primate retina contains two types of ganglion cells, with high and low contrast sensitivity. Proc Natl Acad Sci U S A 83:2755–2757.
Kaskan P, Franco C, Yamada E, Silveira LCL, Darlington R, Finlay BL. 2005. Peripheral variability and central constancy in mammalian visual system evolution. Proc Biol Sci 272:91–100.

Krubitzer L, Campi KL, Cooke DF. 2011. All rodents are not the same: a modern synthesis of cortical organization. Brain Behav Evol 78:51–93.

Loskota W, Lomax P, Verity M. 1974. A stereotaxic atlas of the Mongolian gerbil brain (Meriones unguiculatus). Ann Arbor, MI: Ann Arbor Science.

Mai JK, Berger K, Sofroniew MV. 1993. Morphometric evaluation of neurophysin-immunoreactivity in the human brain: pronounced inter-individual variability and evidence for altered staining patterns in schizophrenia. J Hirnforsch 34:133–154.

Malpeli JG, Lee D, Baker FH. 1996. Laminar and retinotopic organization of the macaque lateral geniculate nucleus: magnocellular and parvocellular magnification functions. J Comp Neurol 375:363–377.

Mancuso K, Hauswirth WW, Li Q, Connor TB, Kuchenbecker JA, et al. 2009. Gene therapy for red-green colour blindness in adult primates. Nature 461:784–787.

Mollon JD. 1991. Uses and evolutionary origins of primate colour vision. In: Cronly-Dillon JR, Gregory RL, editors. Vision and visual dysfunction, vol 2. Evolution of the eye and visual system. Houndmills, United Kingdom: MacMillan. p 306–319.

Morin L, Wood R. 2001. A stereotaxic atlas of the golden hamster brain. New York: Elsevier.

Neitz J, Carroll J, Yamauchi Y, Neitz M, Williams DR. 2002. Color perception is mediated by a plastic neural mechanism that is adjustable in adults. Neuron 35:883–892.

Olshausen BA, Field DJ. 1996. Emergence of simple-cell receptive field properties by learning a sparse code for natural images. Nature 381:607–609.

Pagel M. 1999. Inferring the historical patterns of biological evolution. Nature 401:877–884.

Papia MF, Burke MW, Zangenehpour S, Palmour RM, Ervin FR, Ptito M. 2010. Reduced soma size of the M-neurons in the lateral geniculate nucleus following foetal alcohol exposure in non-human primates. Exp Brain Res 205: 263–271.

Paxinos G. 2004. The rat brain in stereotaxic coordinates. New York: Elsevier.

Perry A, Cowey A. 1985. The ganglion cell and cone distributions in the monkey's retina: implications for central magnification factors. Vis Res 25:1795–1810.

Perry VH, Silveira LCL. 1988. Functional lamination in the ganglion cell layer of the macaque's retina. Neuroscience 25:217–223.

Picanço-Diniz CW, Silveira LCL, de Carvalho MSP, Oswaldo-Cruz E. 1991. Contralateral visual field representation in area 17 of the cerebral cortex of the agouti: a comparison between cortical magnification factor and retinal ganglion cell distribution. Neuroscience 44:325–333.

Rakic P. 1977. Genesis of the dorsal lateral geniculate nucleus in the rhesus monkey: site and time of origin, kinetics of proliferation, routes of migration and pattern of distribution of neurons. J Comp Neurol 176:23–52.

Reep R, Darlington RB, Finlay BL. 2007. The limbic system in mammalian brain evolution. Brain Behav Evol 70:57–70.

Reese BE. 1988. "Hidden lamination" in the dorsal lateral geniculate nucleus: the functional organization of this thalamic region in the rat. Brain Res 13:119–137.

Robinson SR. 1987. Ontogeny of the area centralis in the cat. J Comp Neurol 255:50–67.

Ross CF. 2000. Into the light: the origin of Anthropoidea. Annu Rev Anthropol 29:147–94.

Rowe N, Mittermaier RA. 1996. The pictorial guide to living primates. Charlestown, RI: Pogonias Press.

Rylands AB, Mittermeier RA. 2009. The diversity of the New World primates (Platyrrhini). In: Garber PA, Estrada A, Bicca-Marques JC, Heymann EW, Strier KB, editors. South American primates: comparative perspectives in the study of bahavior, ecology, and conservation. New York: Springer. p 23–54.

Schulz H-D. 1967. Metrische untersuchungen an den schichten des corpus geniculatum laterale tag- und nachtaktiver primaten. PhD thesis, Johann Wolfgang Goethe-Universitat Frankfurt.

Seecharan DJ, Kulkarni AL, Lu L, Rosen GD, Williams RW. 2003. Genetic control of interconnected neuronal populations in the mouse primary visual system. J Neurosci 23:11178–11188.

Selemon LD, Begovic A. 2007. Stereologic analysis of the lateral geniculate nucleus of the thalamus in normal and schizophrenic subjects. Psychiatry Res 151:1–10.

Shapley, RM and Perry, VH. 1986. Cat and monkey ganglion cells and their visual functions roles. Trends Neurosci 9:229–235.

Silveira LCL, Perry VH. 1991. The topography of magnocellular projecting ganglion cells (M-ganglion cells) in the primate retina. Neuroscience 40:217–237.

Silveira LCL, Pincanco-Diniz CW, Sampaio LFS, Oswaldo-Cruz E. 1989. Retinal ganglion cell distribution in the cebus monkey: a comparison with the cortical magnification factors. Vis Res 29:1471–1483.

Silveira LCL, Perry VH, Yamada ES. 1993. The retinal ganglion cell distribution and the representation of the visual field in area 17 of the owl-monkey Aotus trivirgatus. Vis Neurosci 10:887–897.

Silveira LC, Yamada ES, Perry VH, Picanco-Diniz CW. 1994. M and P retinal ganglion cells of diurnal and nocturnal New-World monkeys. Neuroreport 5:2077–2081.

Singer W. 1977. Control of thalamic transmission by corticofugal and ascending reticular pathways in the visual system. Physiol Rev 57:386–420.

Song S, Liu L, Edwards SV, Wu S. 2012. Resolving conflict in eutherian mammal phylogeny using phylogenomics and the multispecies coalescent model. Proc Natl Acad Sci U S A 109:14942–14947.

Stephan H, Frahm H, Baron G. 1981. New and revised data on volumes of brain structures in insectivores and primates. Fol Primatol 35:1–29.

Stone J. 1983. Parallel processing in the visual system. New York: Plenum Press.

Suner I, Rakic P. 1996. Numerical relationship between neurons in the lateral geniculate nucleus and primary visual cortex in macaque monkeys. Vis Neurosci 13:585–590.

Van Essen DC, Newsome WT, Maunsell JH. 1984. The visual field representation in striate cortex of the macaque monkey: asymmetries, anisotropies, and individual variability. Vis Res 24:429–448.

Van Essen DC, Glasser MF, Dierker DL, Harwell J. 2012. Cortical parcellations of the macaque monkey analyzed on surface-based atlases. Cereb Cortex 22:2227–2240.

Wässle H, Grünert U, Röhrenbeck J, Boycott BB. 1989. Cortical magnification factor and the ganglion cell density of the primate retina. Nature 341:643–646.

Wässle H, Grünert U, Röhrenbeck J, Boycott, BB. 1990. Retinal ganglion cell density and cortical magnification factor in the primate. Vis Res 30:1897–1990.

Williams AL, Jeffery G. 2001. Growth dynamics of the developing lateral geniculate nucleus. J Comp Neurol 430:332–342.

Williams D, Sekiguchi N, Brainard D. 1993. Color, contrast sensitivity, and the cone mosaic. Proc Nat Acad Sci U S A 90:9770–9777.

Williams RW, Rakic P. 1988. Elimination of neurons from the lateral geniculate nucleus of rhesus monkeys during development. J Comp Neurol 272:424–436.

Workman AD, Charvet CJ, Clancy B, Darlington RB, Finlay BL. 2013. Modeling transformations of neurodevelopmental sequences across mammalian species. J Neurosci 33: 7368–7383.

Yamada ES, Silveira LCL, Perry VH. 1996. Morphology, dendritic field size, somal size, density, and coverage of M and P retinal ganglion cells of dichromatic cebus monkeys. Vis Neurosci 13:1011–1029.

Yamada ES, Silveira LCL, Perry VH, Franco ECS. 2001. M and P retinal ganglion cells of the owl monkey: morphology, size and photoreceptor convergence. Vis Res 41:119–131.

Yom-Tov Y. 1993. Does the rock hyrax, Procavia capensis, conform with Bergmann's rule? Zool J Linnean Soc 108: 171–177.

Yopak KE, Lisney TJ, Darlington RB, Collin SP, Montgomery JC, Finlay BL. 2010. A conserved pattern of brain scaling from sharks to primates. Proc Natl Acad Sci U S A 107: 12946–12951.